EISEVIED

Contents lists available at ScienceDirect

# Palaeogeography, Palaeoclimatology, Palaeoecology

journal homepage: www.elsevier.com/locate/palaeo



Invited Research Article



# Application of cave monitoring to constrain the value and source of detrital $^{230}$ Th/ $^{232}$ Th in speleothem calcite: Implications for U-series geochronology of speleothems

Barbara E. Wortham a,\*, Jay L. Banner b, Eric W. James b, R. Lawrence Edwards c, Staci Loewy b

- a Department of Earth and Planetary Science, University of California, Berkeley, 307 McCone Hall, Berkeley, California, United States of America
- b Department of Geological Sciences, University of Texas at Austin, 1 University Station, Austin, TX, 78712, United States of America
- <sup>c</sup> Department of Earth and Environmental Science, University of Minnesota, Minneapolis, MN, United States of America

ARTICLE INFO

Editor: Shucheng Xie

Keywords: Stalagmites Cave monitoring U-series dating

#### ABSTRACT

Cave calcite deposits ("speleothems") are widely-used archives of terrestrial paleoclimate signals, in large part because they can be accurately and precisely dated using <sup>238</sup>U-series disequilibria (U-series dating) measured by mass spectrometry. Difficulties arise when growth layers in stalagmites incorporate detrital material during calcite deposition that contains significant amounts of <sup>230</sup>Th ("detrital <sup>230</sup>Th"). U-series ages must be corrected for detrital  $^{230}$ Th either by 1) assuming a detrital  $^{230}$ Th content (expressed as the ratio  $^{230}$ Th/ $^{232}$ Th), or by 2) developing isochron models for each stalagmite. We examine two alternative correction approaches for detrital  $^{230}$ Th/ $^{232}$ Th: analysis of calcite grown on artificial substrates in central Texas caves (i.e., present-day or "zeroage" calcite) and analysis of soil leachates from the recharge zones of the caves. Samples collected over three years yield elevated detrital atomic  $^{230}$ Th/ $^{232}$ Th values, ranging from 5.4 to 28.1 parts per million (ppm)  $\pm$  0.5 ppm ( $1\sigma$  uncertainty for a typical measurement), compared with the commonly used "bulk earth" value of 4.4 ppm. Agreement between soil leachate and calcite <sup>230</sup>Th/<sup>232</sup>Th values suggests that soil material is a source of detrital Th in the stalagmites in central Texas. Correlations between Fe, Mn, and Th concentrations in soil leachates from above caves suggests that Th sorbs on to Fe and Mn colloidal material. Independent estimates of detrital  $^{230}$ Th/ $^{232}$ Th in a young (< 100 years) stalagmite from central Texas reveal higher  $^{230}$ Th/ $^{232}$ Th (~4 to 11 ppm) than bulk earth, consistent with measurements from zero-age calcite and soil (~5 to 20 ppm). These results offer a new method for improving U-series chronologies of stalagmites.

#### 1. Introduction

The utility of speleothem proxy time series is dependent on the accuracy and precision of the <sup>238</sup>U-series disequilibrium dating method (Useries) (Edwards et al., 1987, 1993; Cheng et al., 2000, 2013; Musgrove et al., 2001; McDermott, 2004; Wong and Breecker, 2015; Wendt et al., 2021). U-series dating involves measuring the concentrations of <sup>238</sup>U, and the intermediate daughter products of <sup>238</sup>U decay, <sup>234</sup>U and <sup>230</sup>Th (e.g., Edwards et al., 1987; Schwarcz and Latham, 1989; Zhao et al., 2009; Richards and Dorale, 2003). Stalagmite geochronology based on <sup>238</sup>U decay assumes that essentially all of the daughter product (<sup>230</sup>Th) that is measured in a sample is from the decay of <sup>234</sup>U (Richards and Dorale, 2003; Wendt et al., 2021). However, stalagmites can incorporate detritus containing Th during deposition or can incorporate Th into the

mineral lattice (Przybylowicz et al., 1991; Labonne et al., 2002; Zhao et al., 2009; Blyth et al., 2015) as do some pedogenic silica-carbonates (e.g., Ludwig and Paces, 2002). Such Th inclusion in stalagmite calcite introduces uncertainties to measured ages that may be large relative to the instrumental errors of the U-series isotope measurements (Fig. 1). The <sup>230</sup>Th concentration measured in stalagmite calcite ([<sup>230</sup>Th]<sub>measured</sub>) thus has two sources, <sup>230</sup>Th from the radioactive decay of <sup>234</sup>U ("[<sup>230</sup>Th]<sub>radiogenic</sub>" hereafter) since deposition and <sup>230</sup>Th that was incorporated at the time of deposition ("[<sup>230</sup>Th]<sub>detrital</sub>") (Eq. 1).

$$\begin{bmatrix}
^{230}\text{Th}\end{bmatrix}_{\text{measured}} = \begin{bmatrix}
^{230}\text{Th}\end{bmatrix}_{\text{radiogenic}} + \begin{bmatrix}
^{230}\text{Th}\end{bmatrix}_{\text{detrital}}$$
(1)

Correction for detrital  $^{230}$ Th (Eq. (1)) in calcite requires the measurement of  $^{232}$ Th and knowledge of the  $^{230}$ Th/ $^{232}$ Th ratio of the detritus (herein referred to as detrital  $^{230}$ Th/ $^{232}$ Th ratio). There are two

E-mail address: babswortham@berkeley.edu (B.E. Wortham).

<sup>\*</sup> Corresponding author.

correction techniques. The first assumes the detrital component has the estimated bulk earth  $^{230}{\rm Th}/^{232}{\rm Th}$  value of 4.4 ppm. This value is obtained using 1) an empirically derived average for Th/U in terrestrial upper continental crust that ranges from 3.6 to 3.8, as the source of detritus (Taylor and McLennan, 1995; Wedepohl, 1995), and 2) the assumption that the detrital component is sufficiently old such that  $^{230}{\rm Th}$  is in secular equilibrium with  $^{238}{\rm U}$  in this source (Zhao et al., 2009; Richards and Dorale, 2003). Using this method, variability in the detrital  $^{230}{\rm Th}/^{232}{\rm Th}$  can impact age uncertainty in stalagmites (Fig. 1). Uncertainty in stalagmite ages increase 1) with increasing measured  $^{232}{\rm Th}/^{238}{\rm U}$  (Fig. 1A), or 2) with decreasing stalagmite age for a given  $^{232}{\rm Th}/^{238}{\rm U}$ . In the latter case, as stalagmite age decreases the contribution from detrital  $^{230}{\rm Th}/^{238}{\rm U}$  (Fig. 1B; Eq. (1)). The bulk earth assumption is not problematic for samples in which the  $^{232}{\rm Th}/^{238}{\rm U}$  ratio

is small and/or the stalagmite is old enough to allow the in-growth of large amounts of radiogenic <sup>230</sup>Th relative to detrital <sup>230</sup>Th (Eq. (1); Fig. 1). Additionally, the bulk earth assumption is commonly applied with an assumed uncertainty of 50–100% (Table 1). Notably, these bulk earth uncertainties can propagate to large stalagmite age uncertainties in young stalagmites. Alternatively, the absolute value of the analytical uncertainty in U-series ages increases with age, such that the contribution to the age uncertainty from the uncertainty associated with bulk earth assumption decreases with age (Fig. 1). Propagation of this uncertainty associated with the value of the bulk earth assumption is illustrated in Fig. 1A and B (Supp. Material). Uncertainty in estimating detrital <sup>230</sup>Th/<sup>232</sup>Th and its impact on the uncertainty of calculated U-series ages is especially relevant for young stalagmites, as represented by a suite of stalagmites aged 0 to 60 ka (Table 1; Fig. 1A, B, and C). For stalagmites of any age that are detrital-rich ('dirty'), the detrital

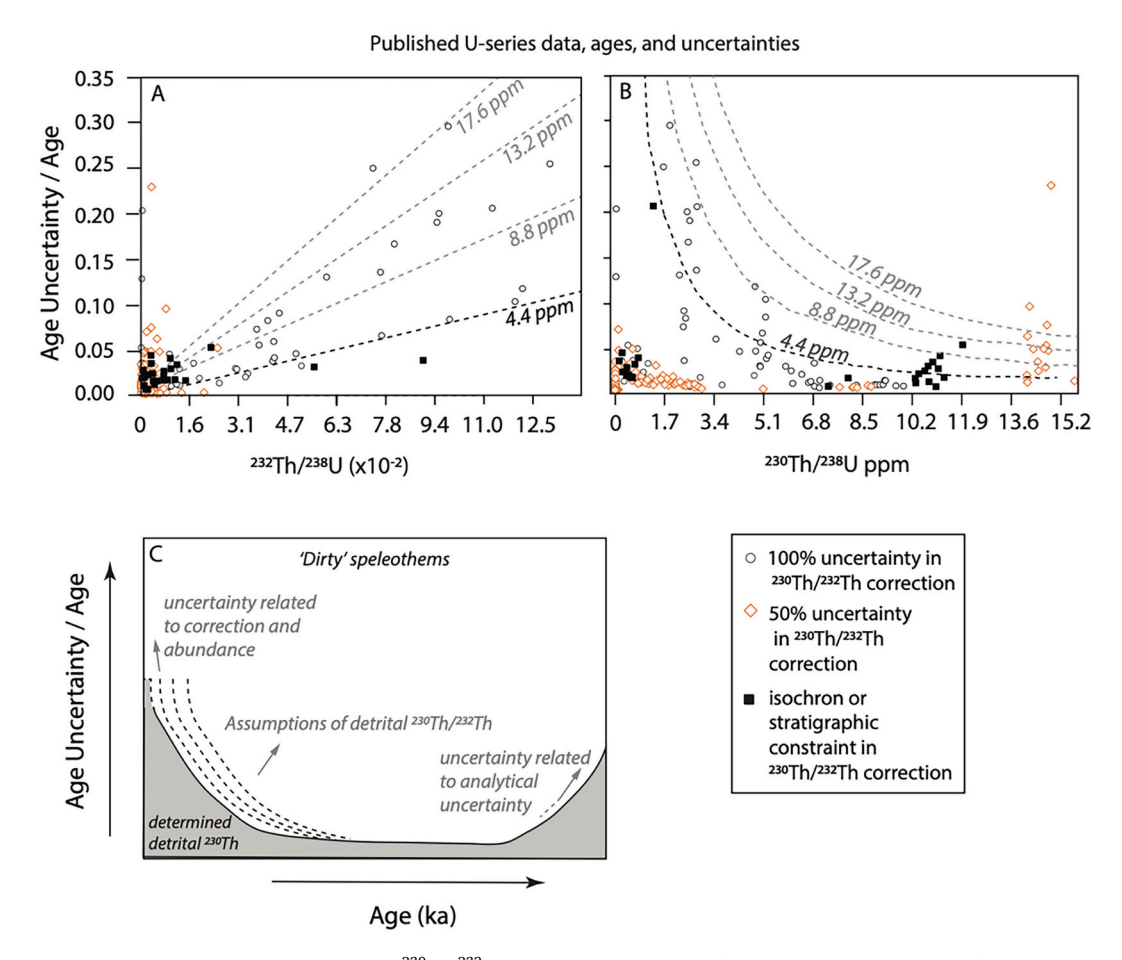


Fig. 1. Diagram of the contribution of the estimated detrital <sup>230</sup>Th/<sup>232</sup>Th assumption to the overall uncertainty on the age in relation to the measurement of (A) <sup>232</sup>Th/<sup>238</sup>U, (B) <sup>230</sup>Th/<sup>238</sup>U, and an illustration of the impact on absolute age (C). (A and B) Contours are theoretical and data points are measurements on stalagmites from the literature. Contours represent a calculated relationship between age uncertainty and (A) <sup>232</sup>Th/<sup>238</sup>U and (B) <sup>230</sup>Th/<sup>238</sup>U over variable <sup>230</sup>Th/<sup>232</sup>Th values. Notably, the calculations for the contours must use constant values for some pieces of the age equation to evaluate the contribution to age uncertainty from the detrital <sup>230</sup>Th/<sup>232</sup>Th (constants given in Table S1). Alternatively, data points (A and B) represent the measured relationship between age uncertainty and (A) <sup>232</sup>Th/<sup>238</sup>U and (B) <sup>230</sup>Th/<sup>238</sup>U in various stalagmites in the literature. The data points reveal a more nuanced story with the uncertainty assigned to detrital <sup>230</sup>Th/<sup>232</sup>Th value playing a role in the age uncertainty noted in this diagram as illustrated by the larger age uncertainty in both A and B for data that use 100% uncertainty with the detrital 230Th/232Th assumption. In combination, the contours and the data points show the contribution that both the value of the detrital <sup>230</sup>Th/<sup>232</sup>Th (contours) and the uncertainty assigned to that value (data points) have on the uncertainty of ages from stalagmites. The bulk earth value of 4.4 ppm is highlighted as a black dashed line. With increasing value of estimated detrital <sup>230</sup>Th/<sup>232</sup>Th used in age calculations, age uncertainty increases in relation to the <sup>232</sup>Th/<sup>238</sup>U (A) and <sup>230</sup>Th/<sup>238</sup>U (B). Age uncertainty is highest for high <sup>232</sup>Th/<sup>238</sup>U values, reflecting samples with a high detrital component and/or low U. Previously published data are presented as published (Musgrove et al. (2001); Hellstrom (2006); Wong et al. (2015); Zhao et al. (2009); Hardt et al. (2010); Meckler et al. (2012, 2015); Lachniet et al. (2014); Denniston et al. (2013); Carolin et al. (2016).) For illustration purposes only, C represents an idealized schematic of the relationship between age uncertainty and age in a stalagmite based on current understanding of the relative contributions of uncertainties in U-series measurements. The increased uncertainty related to the estimate of detrital <sup>230</sup>Th/<sup>232</sup>Th is crucial for younger samples (<50-60 ka based on the data used here) whereas the uncertainty related to analytical measurements is increasingly important in older samples (>120 ka based on the data used here). The dashed lines indicate different theoretical amounts of detrital Th incorporated in a detrital rich or "dirty" speleothem.

Table 1 Previously published values of initial  $^{230}$ Th.\*

	<sup>230</sup> Th/ <sup>232</sup> Th (ppm)	Uncertainty (%) <sup>a</sup>
Commonly assumed initial values	1.5 to 4.4	50 to 100%
Moseley et al., 2014 (Isochron)	2.4 to 17.3	50%
Carolin et al., 2016 (Isochron)	55 to 127	9 to 50%
James, 2017 (Isochron)	14.7	25%
Labonne et al., 2002 (Isochron)	3.1 to 3.2	13 to 17%
Polyak et al., 2004 (Isochron)	5 to 60	50%
Scroxton et al., 2016 (Stratigraphic Constraint		
Modeling (common method): code from Hellstrom (2006))	16.2	25%
Lachniet et al., 2014 (Isochron)	8.6 to 15	50%
Denniston et al., 2013 (Isochron not used for age calculation)	2.4	17%

<sup>\*</sup> Refs: Banner et al., 2007; Dorale et al., 2004; Musgrove et al., 2001; Wagner et al., 2010; Hardt et al., 2010; Novello et al., 2012; Cai et al., 2017; Denniston et al., 2013; Steponaitis et al., 2015; Lachniet et al., 2014; Oster et al., 2020.

 $^{230} {\rm Th}/^{232} {\rm Th}$  value must be well constrained to reduce U-series age uncertainty (Fig. 1D). The large range of assumed uncertainty used for the bulk earth detrital estimate ( $\pm\,50{-}100\%$ ) reflects the difficulty of using a single value to represent all variability in the composition of detritus from different terrestrial environments (Taylor and McLennan, 1995; Wedepohl, 1995). An incorrect assignment of the detrital  $^{230} {\rm Th}/^{232} {\rm Th}$  value, regardless of the uncertainty, has a large impact on the correction to the measured  $^{230} {\rm Th}/^{238} {\rm U}$  values used in calculating ages. Thus, both using an accurate value of detrital  $^{230} {\rm Th}/^{232} {\rm Th}$  and minimizing the uncertainty associated with that value are important to constrain accurate ages (Fig. 1).

The second approach to correct for detrital <sup>230</sup>Th/<sup>232</sup>Th is to subsample and analyze a single growth layer in a stalagmite to calculate an isochron that provides a more precise estimate of detrital <sup>230</sup>Th/<sup>232</sup>Th (Table 1). This method yields a reduced uncertainty of the age model (Fig. 1A & B) and an accurate estimate of the detrital <sup>230</sup>Th/<sup>232</sup>Th values for this layer. The isochron method, however, is time and material intensive and is sometimes unsuccessful because multiple Th sources can complicate isochron interpretation (Lin et al., 1996; Richards and Dorale, 2003; Denniston et al., 2013). In summary, complications in applying U-series dating to stalagmites that are detritus-rich and/or young may lead to excluding such samples for paleoclimate reconstructions, highlighting the need for developing additional or improved methods to correct for detrital <sup>230</sup>Th.

We propose a novel method of characterizing and correcting for detrital  $^{230}{\rm Th}/^{232}{\rm Th}$  in speleothems by measuring the  $^{230}{\rm Th}/^{232}{\rm Th}$  ratio in soils and in zero-age calcite grown on artificial substrates in modern cave settings. We demonstrate that zero-age calcite  $^{230}{\rm Th}/^{232}{\rm Th}$  ratios measured in this study are elevated in comparison to the bulk earth value and that the measured values agree with an independent estimation of detrital  $^{230}{\rm Th}/^{232}{\rm Th}$  in a stalagmite from one of the same caves (WC3; Carlson et al., 2018). This study is particularly relevant for speleothem samples of Holocene age and samples that have a high concentration of detrital material (commonly referred to as 'dirty' speleothems). The source of high detrital  $^{230}{\rm Th}/^{232}{\rm Th}$  values in calcite from one site is the overlying soil, based on measurements of  $^{230}{\rm Th}/^{232}{\rm Th}$  in calcite and in soil, and the Th, Fe and Mn concentrations in cave calcite and soil.

## 2. Hydrogeologic setting

We focus on three central Texas caves: Natural Bridge Caverns (NB), Inner Space Cavern (IS), and Westcave Preserve (WC) (Musgrove and Banner, 2004; Banner et al., 2007; Wong et al., 2011; Casteel and Banner, 2015; Feng et al., 2014). All three caves are developed within the

Edwards Plateau, a karstified carbonate platform of lower Cretaceous age (Elliot and Veni, 1994; Fig. 2). Cave NB is located within both the upper Glen Rose Limestone and the Walnut formation of the Edwards Group Cretaceous limestones (Musgrove and Banner, 2004; Cowan et al., 2013). Cave IS is formed solely in Edwards Formation (Kastning, 1983; Banner et al., 2007) and WC is formed in the Cow Creek formation (Casteel and Banner, 2015).

The climate of the Edwards plateau has decreasing precipitation from east to west (Larkin and Bomar, 1983) with a 30-year normal precipitation for Comal, Travis, and Williamson Counties (counties containing NB, WC, and IS, respectively) ranging from 71 to 81 cm/year (PRISM Climate Group, 2015a). The seasons amount to dry, hot summers, wetter springs and falls, and dry, mild winters, with a 30-year normal temperature ranging from 17 to 22 °C (PRISM Climate Group, 2015b). Central Texas is generally prone to droughts with intermittent wet periods (Banner et al., 2007). The sampling period of 2012 to 2013 was considered a time of moderate to severe drought (Climate Prediction Center (CPC), 2015).

Two of the three cave systems (NB and IS) are "deep" caves that experience near-constant cave temperatures and seasonal variability in cave-air  $pCO_2$  (Banner et al., 2007; Wong et al., 2011; James et al., 2015). In NB and IS,  $CO_2$  rises during the summer when surface air temperature is greater than cave-air temperature, resulting in a decrease to cessation of calcite precipitation (Banner et al., 2007; Wong et al., 2011; James et al., 2015). In contrast, WC is ventilated year-round as a result of the cave morphology. WC has a small internal volume and a large opening area that leads to a small opening area to volume ratio of  $\sim 0.02 \, \mathrm{m}^{-1}$  (Feng et al., 2014; Cowan et al., 2013). The cave morphology at WC allows for cave-air  $pCO_2$  to remain near atmospheric values leading to calcite growth throughout the year (Casteel and Banner, 2015; Carlson et al., 2018) in contrast to the seasonality in calcite growth observed at NB and IS.

## 3. Methods

To characterize the detrital <sup>230</sup>Th/<sup>232</sup>Th value of actively growing calcite, we primarily sampled calcite grown on artificial substrates for monthly intervals from 2012 to 2013 at all three caves. Additionally, we subsampled two artificial substrates that were deployed in WC in 2010 and were retrieved as part of this study in 2012. The artificial (glass) substrates are etched, acid cleaned, microscopically inspected prior to deployment, and then sampled under a binocular microscope taking precaution to avoid the glass surface while sampling the calcite. We used two different types of plates for two different intervals of time. First, we used cleaned watch-glasses (curved plates) that were placed at sites WC-C1 and WC-C2 for two years (2010-2012; Fig. 2) and were collected in the summer of 2012. In the summer of 2012, we switched to 20 cm  $\times$  20 cm flat plates. The flat plates were placed under active drip-sites (n = 2at WC, n = 1 at NB, n = 2 at IS) at the caves for approximately four weeks at a time between the summer of 2012 and the summer of 2013 (Fig. 2). All plates were placed horizontally under active drip-sites. Calcite grown on each substrate ('zero-age calcite' hereafter) was collected following the protocol of Banner et al. (2007). Cave IS drip-sites (Fig. 2) used in this study were previously characterized by Casteel (2011) and Hulewicz (2012) and demonstrated regular calcite growth during the year. In previous publications these sites were named ISS3 and ISS4.

After calcite substrate collection, selected areas of each plate were gently scraped under the binocular microscope with an acid-cleaned stainless-steel tool to remove the calcite for U-series measurements (Table 2). Each calcite sample was dissolved, and chemical separation of U and Th was completed using iron co-precipitation and ion exchange chemistry in the Isotope Clean Lab at University of Texas, Austin (Musgrove et al., 2001; Wong et al., 2015). <sup>230</sup>Th/<sup>232</sup>Th ratios were measured using a ThermoScientific Triton thermal ionization mass-spectrometer (4 calcite samples) (Musgrove et al., 2001; Wong et al., 2011) at University of Texas, Austin (UT) and using a ThermoScientific

 $<sup>^{\</sup>rm a}$  Uncertainty percentages are calculated from the  $\pm$  uncertainty reported in each citation.

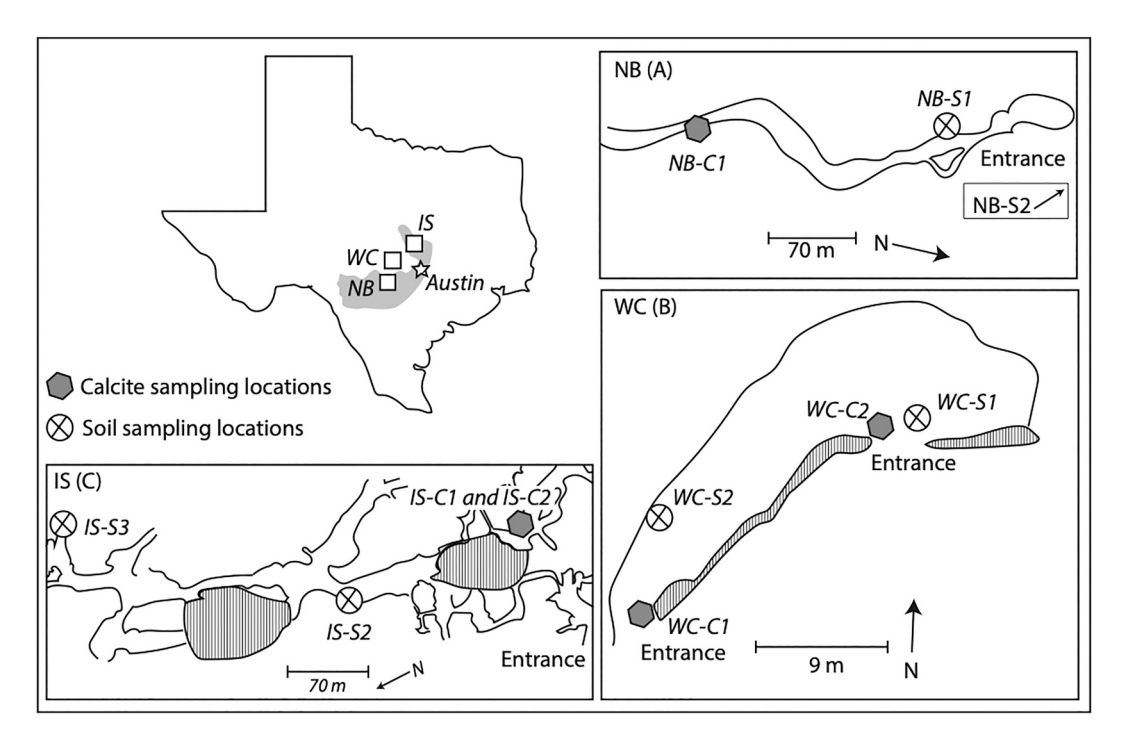


Fig. 2. Central Texas maps (A-C) are within the Edwards Aquifer and Recharge Zone (grey shaded region). Maps of the caves are generalized to illustrate the relative location of soil samples and calcite samples, modified from Musgrove and Banner (2004) and Casteel (2011). (A) Natural Bridge South Cave (NB) is the southern most cave. The NB calcite sampling location (crossed circle; NB-C1) is ~240 m from the entrance of the cave and was chosen to be near one of the previously sampled soil (grey hexagon; NB-S1 and NB-S2; Musgrove and Banner, 2004). Soil sample NB-S2 is above the north cave at NB off of the scope of the map. (B) Westcave Preserve (WC) is a small cave with a large entrance to cave volume ratio (Cowan et al., 2013), calcite samples (WC-C1 and WC-C2) were taken near entrances and soil samples (WC-S1 and WC-S2) were taken directly above them. Lined filled regions in WC indicate cave walls (C) Inner Space Cavern (IS) is the northern most cave of this study, calcite samples (IS-C1 and IS-C2) are ~300 m from the entrance and soil samples (Musgrove and Banner, 2004) are at locations above the cave (IS-S2 and IS-S3). Line filled regions indicate cave fill.

Table 2
Calcite measurements.

Measured at UM							
Sample name	Sample location	<sup>232</sup> Th		<sup>230</sup> Th		<sup>230</sup> Th/ <sup>232</sup> Th	
		pg/g	1 SE abs	fg/g	1 SE abs	Atomic ppm	1 SE abs
WC-13	WC-C1	9500	±52	65.7	±4.1	7	±0.4
B03	WC-C1	10,121	$\pm 39$	185.7	±4.4	18.5	$\pm 0.4$
WC-B04	WC-C2	3851	$\pm 14$	78.1	$\pm 2.1$	20.5	$\pm 0.5$
WC-B04-R	WC-C2*	3859	$\pm 11$	80.2	$\pm 2.2$	21	$\pm 0.6$
WC-14	WC-C2	5973	$\pm 21$	32	$\pm 2.7$	5.4	$\pm 0.5$
IS- 1428	IS-C1	9577	$\pm 32$	267	±4.4	28.1	$\pm 0.5$
IS- 1430	IS-C2	12,402	±44	233.7	±5.7	19	$\pm 0.5$
IS -1444	IS-C2	17,684	$\pm 58$	423.7	$\pm 7.9$	24.2	$\pm 0.5$
NB- 1458	NBC1	10,560	$\pm 41$	171.1	$\pm 4.8$	16.3	$\pm 0.5$
NB 1400	NBC1	2689	$\pm 10$	48.3	$\pm 1.6$	18.1	$\pm 0.6$
NB- 1400R	NBC1*	2703	$\pm 8$	47.8	$\pm 1.7$	17.8	$\pm 0.6$
Measured at UT							
BO2Big	WC-C1	_	_	_	_	15.3	$\pm 0.7$
BO2Small	WC-C1	_	_	_	_	14.6	$\pm 0.8$
WC13Big	WC-C1	_	_	_	_	5.96	$\pm 0.6$
WC14small	WC-C2	_	_	_	_	5.8	$\pm 0.6$

Neptune multi-collector inductively coupled plasma mass spectrometer (12 calcite samples) (MC-ICP-MS; Shen et al., 2002) at the University of Minnesota (UM; Edwards et al., 1987, 1993; Table 1; Fig. 2).

The typical blank for  $^{232}\text{Th}$  is  $1\pm1.6$  pg for measurements at UT Austin. Blank measurements for  $^{230}\text{Th}$  are not performed because the  $^{230}\text{Th}$  signal of the blank is indistinguishable from the ion counter dark noise of 0.02 counts per second (cps). Dark noise is the background signal of the detector and independent of specific masses being analyzed. The ratio of the calculated mass of  $^{230}\text{Th}$  ionized from the

filament (assuming 1% ionization efficiency) to measured  $^{230}\text{Th}$  signal intensity is 0.3 fg/cps. Accordingly, the 0.02 cps dark noise corresponds to 6 ag, a maximum estimate for  $^{230}\text{Th}$  analytical blank. Five analyses of the in-house standard ('White Flowstone') using the ThermoScientific Triton thermal ionization mass-spectrometer, a Micromass Isoprobe Multicollector Inductively Coupled Plasma Mass-Spectrometer, and a MAT 261 Thermal Ionization Mass Spectrometer (all at UT Austin) yielded a  $^{230}\text{Th}$  / $^{232}\text{Th}$  ratio of 2.09  $\pm$  0.01 (1 $\sigma$ ). A long-term conservative estimate of the blank for analyses of  $^{232}\text{Th}$  on calcite at UM is 0.5

 $\pm$  0.5 pg and the blank for analyses of  $^{230}\text{Th}$  is 20  $\pm$  20 ag.

Soil samples at IS and NB were collected previously (site descriptions and data in Musgrove and Banner (2004)) (Fig. 2). The same methods (Musgrove and Banner, 2004) were used at two additional sites at WC (Fig. 3). Each sample (Table 3) was homogenized in a clean plastic bag and split into two portions. The soils were air dried. One portion was leached with 1 M ammonium acetate (AA; pH = 8) three times for 24 h and the soil supernatant was collected and dried (Musgrove et al., 2001) to analyze for AA-exchangeable cations (Bohn et al., 1985). The second portion was leached with 18  $M\Omega$  deionized water (DI; pH 7.57) to flush remaining soil pore water analyze for and dissolve water-soluble salts (Bohn et al., 1985) and water-exchangeable ions. Supernatant from these leachates were separately collected, acidified, and dried. The elemental concentrations of U, Th, Fe, and Mn in each leachate were measured using an Agilent 7500ce quadrupole inductively coupled plasma mass spectrometer at UT Austin. Additionally, the <sup>230</sup>Th, <sup>232</sup>Th, and <sup>238</sup>U of the soil leachates were analyzed using the same methods as described above for the calcite isotopic measurements (Table 3).

#### 4. Results

 $^{230}$  Th/ $^{232}$  Th values in zero-age plate calcite for all three caves range from 5.4 to 28.1  $\pm$  0.5 ppm (Table 2; Fig. 3). WC zero-age calcite  $^{230}$  Th/ $^{232}$  Th values (n=5) range from 5.4 to 21.0 ppm (Table 2, Fig. 3). NB zero-age calcite  $^{230}$  Th/ $^{232}$  Th values (n=2) ranged from 16.3 to 18.1  $\pm$  0.5 ppm and IS calcite (n=3) ranged from 19.0 to 28.1  $\pm$  0.5 ppm (Table 2; Fig. 3). There is not a geographic or temporal trend in the data.

DI water leachates of soils yield a  $^{230}$ Th/ $^{232}$ Th range of 4.5  $\pm$  0.3 to 17.2  $\pm$  0.6 ppm for all three caves (Table 3). The ammonium acetate leachates yield  $^{230}$ Th/ $^{232}$ Th values that range from 5.7  $\pm$  0.6 to 16.4  $\pm$  0.8 ppm (Table 3). The AA soil leachates result in a narrower  $^{230}$ Th/ $^{232}$ Th range than the DI leachates from the same cave (Fig. 4). Soil and zero-age calcite  $^{230}$ Th/ $^{232}$ Th analyses from WC agree within uncertainty. All soil and calcite values are above the bulk earth value of 4.4 ppm, however, the soil  $^{230}$ Th/ $^{232}$ Th values from NB and IS do not agree with the zero-age calcite  $^{230}$ Th/ $^{232}$ Th values at these two sites (Fig. 4).

While elemental concentrations (Th, U, Mn, and Fe) of all the soil samples are routinely higher in DI leaches than AA leaches (Table 3), the  $^{230}\mathrm{Th}/^{232}\mathrm{Th}$  values of both leach types agree (Table 2; Table 3; Fig. 4). Th concentrations at WC strongly correlate with Fe and Mn concentrations in both DI and AA leachates (r² > 0.97, p < 0.05 for all cases; Fig. 4)

and a significant correlation between the Th and U concentration in the AA leachates from WC ( $\rm r^2=0.99,\,p<0.05$ ). There is not a significant correlation between Th concentrations and other trace and major elements (Supp. Table 1).

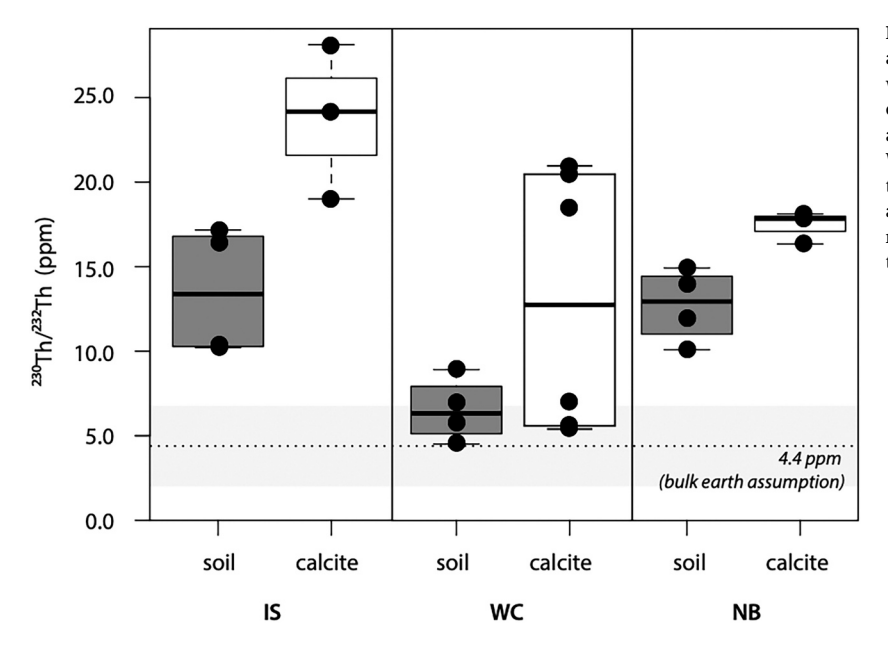
## 5. Discussion

# 5.1. Zero-age calcite <sup>230</sup>Th/<sup>232</sup>Th values

Measurements of atomic <sup>230</sup>Th/<sup>232</sup>Th in zero-age calcite are above the bulk earth value of 4.4 ppm in all central Texas caves measured here and in agreement with other estimates of detrital <sup>230</sup>Th/<sup>232</sup>Th values (Fig. 3; Table 1). These results agree with other studies that report Useries stalagmite dates using isochron methodologies, which find a detrital <sup>230</sup>Th/<sup>232</sup>Th value that is higher than the bulk earth value and that varies through time in each stalagmite (e.g., Labonne et al., 2002; Polyak et al., 2004; Carolin et al., 2016). Moreover, in a central Texas cave not monitored in this study, isochron models estimate detrital  $^{230}$ Th/ $^{232}$ Th values of 14.7 to 20.7 ppm (James, 2017), which is within the range of 5.4 to 28.1 ppm we find for zero-age calcite <sup>230</sup>Th/<sup>232</sup>Th measurements (Fig. 3). Furthermore, Richards et al. (1998) found a  $^{230}$ Th/ $^{232}$ Th value of 81 ppm measured on very young (assumed zeroage) soda straws from Middle Caicos, British West Indies (Richards et al., 1998), suggesting that the detrital <sup>230</sup>Th/<sup>232</sup>Th value in that system is much higher than bulk earth. Results from central Texas and these other studies highlight that the bulk earth value is an average; therefore, it does not always represent the spatial variability inherent in karst systems. Assuming bulk earth <sup>230</sup>Th/<sup>232</sup>Th values can lead to large uncertainties in U-series ages in stalagmite studies (Fig. 1). Understanding the true contribution of detrital <sup>230</sup>Th/<sup>232</sup>Th can significantly improve the uncertainty in U-series ages (Fig. 1). Monitoring for the contribution of detrital <sup>230</sup>Th/<sup>232</sup>Th could improve the uncertainty in age models developed from these caves, and it may also lead to a better understanding of the sources and drivers of variable <sup>230</sup>Th/<sup>232</sup>Th.

# 5.2. Evaluating detrital <sup>230</sup>Th/<sup>232</sup>Th measurements within stalagmite

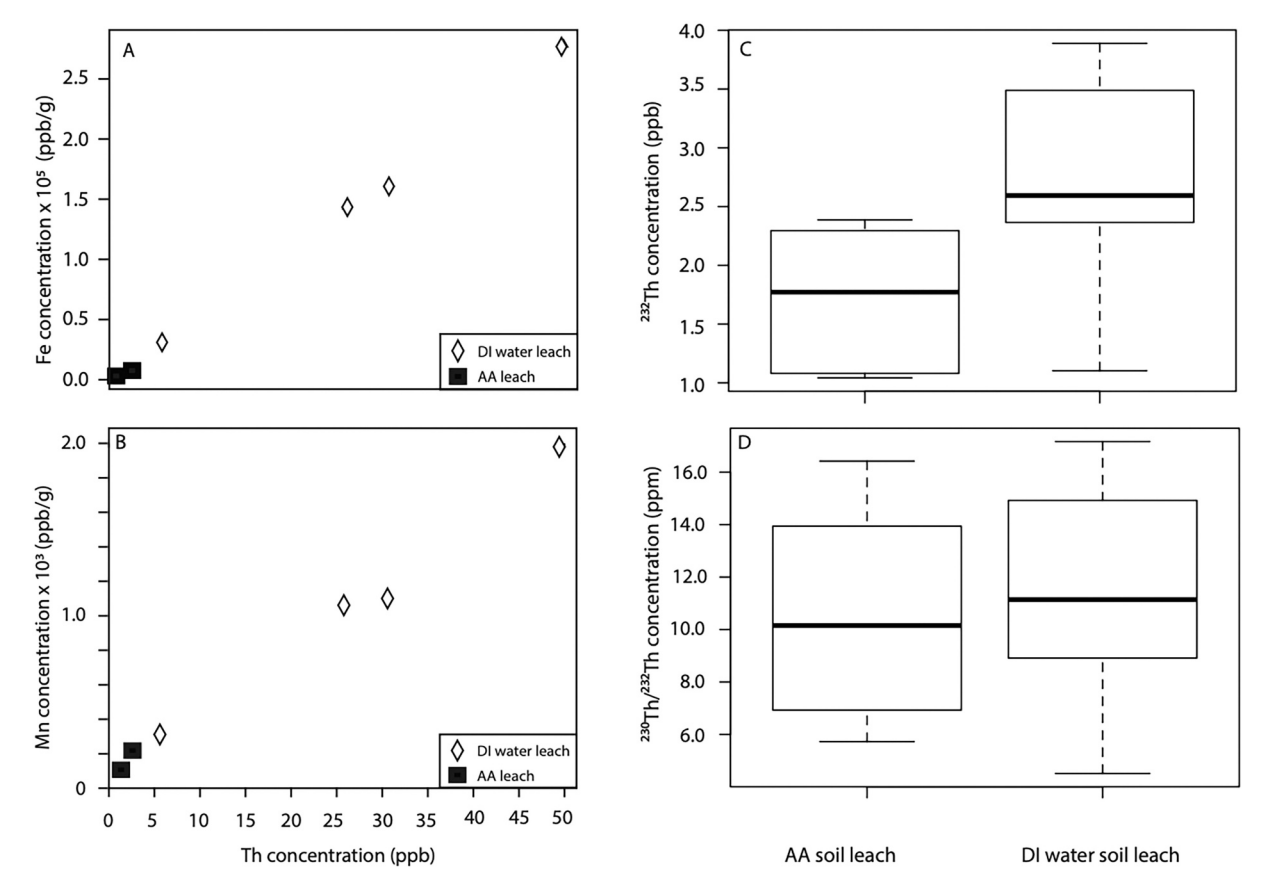
To better assess the measured detrital  $^{230}$ Th/ $^{232}$ Th from WC zero-age calcite, we modeled the detrital  $^{230}$ Th/ $^{232}$ Th values for WC using the U-series measurements (Feng et al., 2014) and independently derived ages (Carlson et al., 2018; Carlson et al., 2019) from stalagmite WC3 (Fig. 5).



**Fig. 3.** Zero-age calcite and soil  $^{230}$ Th/ $^{232}$ Th values. Soil (grey) and calcite (white)  $^{230}$ Th/ $^{232}$ Th values represented as box and whisker plots with individual data points represented as black circles. The bulk earth assumption of 4.4  $\pm$  2.2 ppm is shown as a dashed line and shaded region. Soil and calcite values at WC agree with each other on average are within the uncertainty of the bulk earth value, however, many individual values are above bulk earth. Soil and calcite values at NB and IS do not significantly agree and are both significantly elevated from the bulk earth value.

**Table 3** Soil samples measurements.

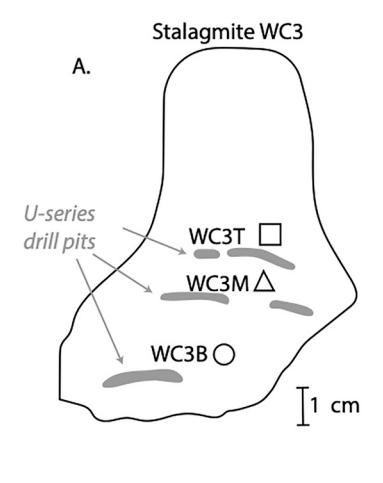
Sample name	Leach type	<sup>232</sup> Th		<sup>230</sup> Th		$^{230}\text{Th}/^{232}\text{Th}$		<sup>238</sup> U	
		pg/g	1 SE abs	fg/g	1 SE abs	atomic ppm	1 SE abs	ng/g	1 SE abs
IS-S2	AA	1080.6	3.4	11.0	0.9	10.2	0.8	4.9	0.1
IS-S2	DI	2364.8	6.4	24.3	1.6	10.3	0.7	6.3	0.0
IS-S3	AA	2295.0	6.7	37.4	1.8	16.4	0.8	5.0	0.0
IS-S3	DI	2781.6	7.5	47.3	1.7	17.2	0.6	2.4	0.0
NB-S1	AA	1388.2	4.5	19.2	1.7	13.9	1.3	3.1	0.0
NB-S1	DI	2406.4	8.4	35.6	1.8	14.9	0.8	3.8	0.0
NB-S2	AA	2386.6	9.3	23.9	1.1	10.1	0.5	3.4	0.0
NB-S2	DI	3488.7	75.1	41.3	2.2	11.9	0.7	1.8	0.0
WC-S1	AA	2156.1	6.2	14.8	1.0	6.9	0.5	0.9	0.0
WC-S1	DI	3888.8	10.1	17.4	1.0	4.5	0.3	1.1	0.0
WC-S2	AA	1042.0	3.0	5.9	0.7	5.7	0.6	1.0	0.0
WC-S2	DI	1102.9	4.1	9.7	1.4	8.9	1.3	0.5	0.0
		Th		Fe		Mn			
Sample Name	Leach type	ppb	1σ (ppb)	ppb	1σ (ppb)	ppb	1σ (ppb)		
WC-S1	AA	1.1	0.02	3489.9	36.1	119.3	0.5		
WC-S1	AA	3.6	0.25	9950.9	141.3	375.8	30		
WC-S1	DI	49.7	0.25	278,615.2	557.2	1987.7	12.7		
WC-S2	DI	26	0.19	144,162.2	562.2	1076	4.8		
WC-S1	DI	30.6	0.17	161,999.5	550.8	1123.9	5.4		
WC-S2	DI	5.7	0.05	32,988.9	112.2	326	2.3		



**Fig. 4.** Soil leach results for both ammonium acetate (AA) and deionized water (DI) leaches. (A) plots of Th concentration vs Fe concentration for AA leaches (black squares) and DI leaches (open diamonds) of WC soils. (B) Same as (A) for Th vs Mn concentration. (C) A box-and-whisker plot showing the <sup>232</sup>Th concentration in soils from NB, IS, and WC for the two leach types. (D) A box-and-whisker plot showing the <sup>230</sup>Th/<sup>232</sup>Th values for the AA and the DI leachates.

Feng et al. (2014) measured three U-series ages for WC3 (90 mm long): two from the middle of the stalagmite (65 and 50 mm from the top; WC3T and M, respectively) and one from the bottom (85 mm, WC3B). The first attempt at U-series dating for WC3, however, was unsuccessful due to the low <sup>230</sup>Th concentrations and, at that time, it was difficult to

constrain the detrital  $^{230}$ Th/ $^{232}$ Th contribution in the stalagmite and cave (Feng et al., 2014). However, Carlson et al. (2018) was able to constrain the age of stalagmite WC3 using the seasonal cycles in the  $\delta^{18}$ O time series. Based on this method, the dates for three growth layers in WC3 are 33, 40, and 49 years BP (top to bottom; Fig. 5; Table 3; Table 4)



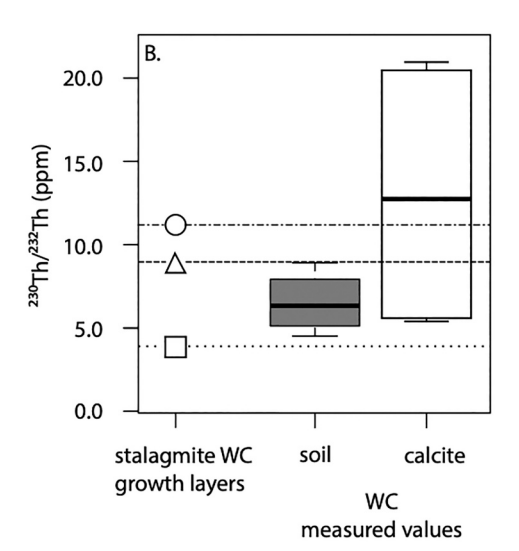


Fig. 5. Schematic of stalagmite WC3 polished slab (Feng et al., 2014; Carlson et al., 2018) illustrating the locations of the original drilled U-series dating pits (A). Values in Table 4. Ages for WC3B (circle), WC3M (triangle), and WC3T (square) were constrained using an age model based on the seasonal cycle of  $\delta^{18}{\rm O}$  in stalagmite calcite, radiocarbon and U-series analyses (Carlson et al., 2018). The  $\delta^{18}{\rm O}$ -cycle ages are and the original U-series data are used to model the detrital  $^{230}{\rm Th}/^{232}{\rm Th}$  for WC3 (Feng et al., 2014). (B) These modeled  $^{230}{\rm Th}/^{232}{\rm Th}$  values are shown in comparison to the soil and calcite measured  $^{230}{\rm Th}/^{232}{\rm Th}$  values. The modeled values for WC3M and WC3B agree with the measured values in this study.

Table 4
Modeled<sup>a</sup> detrital Th.

Sample name	$^{230}$ Th/ $^{232}$ Th modeled (ppm)	$\delta^{18}\text{O-cycle dates (year BP}^{\text{b}})$
WC3B WC3M	11.2 9.0	49 40
WC3T	4.0	33

<sup>&</sup>lt;sup>a</sup> Values were modeled using the U-series measurements from these samples and constrained using the ages estimated by the  $\delta^{18}$ O-cycle (Carlson et al., 2018).

(BP = 2010). The independently derived ages for WC3 allow for the detrital  $^{230}{\rm Th}/^{232}{\rm Th}$  values in WC3 to be calculated. The calculated detrital  $^{230}{\rm Th}/^{232}{\rm Th}$  for the three layers in WC3 are 3.9 ppm (WC3B), 9.0 ppm (WC3M), and 11.2 ppm (WC3T). We consider the  $^{230}{\rm Th}/^{232}{\rm Th}$  values based on the ages from Carlson et al. (2018) to yield independently constrained  $^{230}{\rm Th}/^{232}{\rm Th}$  values and compare them to the measured  $^{230}{\rm Th}/^{232}{\rm Th}$  values of the zero-age calcite from WC (Fig. 5).

The comparison between the independently constrained and calculated detrital  $^{230}{\rm Th}/^{232}{\rm Th}$  values from WC3 and the measurements from zero-age calcite from WC (Fig. 5) highlight two important results: 1) Zero-age calcite is accurately describes the detrital  $^{230}{\rm Th}/^{232}{\rm Th}$  values incorporated in stalagmite calcite from this cave, and 2). Variability in  $^{230}{\rm Th}/^{232}{\rm Th}$  values from zero-age calcite (variable by a factor of 3.8) is captured in stalagmite calcite (variable by a factor of 2.9). These two results suggest that the monitoring of  $^{230}{\rm Th}/^{232}{\rm Th}$  in zero-age calcite can reliably determine the detrital  $^{230}{\rm Th}/^{232}{\rm Th}$  values to use in the U-series dating of stalagmite calcite. Further, the potential variability in  $^{230}{\rm Th}/^{232}{\rm Th}$  values that may impact U-series dating and the ages determined can be captured by the monitoring method described here. Consequently, this method presents an alternative approach to isochron techniques in U-series dating and a more accurate approach to bulk earth assumption techniques.

# 5.3. The source of elevated <sup>230</sup>Th/<sup>232</sup>Th values in calcite

The elevated soil <sup>230</sup>Th/<sup>232</sup>Th values (4.5 to 17.2; Fig. 3) as compared to bulk earth at all three cave sites suggests that soil could be a contributor to the Th incorporated into the zero-age calcite in these systems. We outline a mechanism for this below. Th has a low solubility in natural waters; however, it commonly adsorbs onto clay minerals and humic acids (Morton et al., 2001; Reiller et al., 2002; Nascimento et al., 2019). This absorption allows Th to be mobile in natural waters when

sediment is suspended and transported. For instance, the adsorption of Th to humic acids and clay minerals accounts for up to 90% of Th in the suspended phase of groundwater in Russia (Rachkova et al., 2010). Additionally. The has been shown to rapidly adsorb to suspended particles in marine environments and in saline groundwaters (i.e., Banner et al., 2007). To our knowledge there are no previous studies measuring the amount of Th absorbed to clay minerals or humic acids in central Texas karst systems or cave dripwater. The amount of clay minerals and humic acids in central Texas ground water and cave dripwater, however, has been measured. In the Edwards aquifer, central Texas, clay minerals compose between 30 and 50% of the suspended sediment in groundwater after storm events (Mahler and Lynch, 1999). Because claymineral-rich Edwards aquifer groundwater is part of central Texas karst systems we conclude that it is highly likely there are clay minerals in cave dripwater. Further, it has been shown that luminescence in stalagmites is due to soil-derived fulvic or humic acids (White and Brennan, 1989; Baker et al., 1993, 1997, 1998; Huang et al., 2001; Richards and Dorale, 2003; Orland et al., 2014; Blyth et al., 2015). We note, however, that soil-sourced humic acids are not found in Edwards aquifer well water, potentially because the tortuous flow path in the karst system limits their mobility (Birdwell and Engel, 2009). This discrepancy highlights the need to better understand the relative influence of clay particulates and humic acids on Th transport in central Texas cave systems.

After incorporation in natural waters, Th may co-precipitate with iron and manganese (Fe and Mn) hydroxides (Morton et al., 2001). For instance, Th concentrations are significantly correlated to Fe and Mn in the Ipojuca River of Brazil, both upstream ( $r^2 = 0.62$  and 0.63, p-values <0.05, respectively) and downstream ( $r^2 = 0.66$  and 0.79, p-values <0.05, respectively) of industrial and urban development on the river (e.g. Nascimento et al., 2019). Similar correlations have been observed in streams in China downstream from uranium mines (Wang et al., 2017), and introducing Fe and Mn oxides has been proposed as a way to remove Th from mine tailing discharge (Reiller et al., 2002; Xiu et al., 2019). The correlation of Th concentration in DI and AA leachates to Mn and Fe concentrations (Fig. 3), observed in WC dripwater, suggests that Th is transferred through the karst system to dripwater with clay particulates from central Texas soil and co-precipitates with Fe or Mn (oxy)hydroxides. In summary, the most-likely mechanism for soil to contribute Th to stalagmites is for Th to adsorb on clay minerals in soils, the Th-bearing minerals transported as particulates through the karst system, and the Th precipitates out of solution with iron and/or manganese-oxides. Measurements on dripwater and stalagmite calcite (2 to 90 ka) from Soreq Cave, Israel reveals that high <sup>232</sup>Th in calcite is

<sup>&</sup>lt;sup>b</sup> Year BP indicates 2010.

correlated with Fe, Al, and Si, consistent with Th absorbed to clay particulates that are being transported by drip-water and deposited on stalagmite surfaces (Kaufman et al., 1998). The significant relationship between Th, Fe, and Mn in our study (Fig. 4), and the consistency between the signal observed in caves globally and in Texas, suggests that soil Th is being transferred to stalagmite calcite.

Although the <sup>230</sup>Th/<sup>232</sup>Th values for soil at all three cave sites are elevated compared with bulk earth, the soil and zero-age calcite  $^{230}$ Th/ $^{232}$ Th values agree at WC, but do not at NB and IS (Fig. 3). We suggest that the disagreement between cave calcites and soils at NB and IS, as opposed to WC, may be the result of cave morphology and differences in bedrock between the three sites. NB and IS are 'deep caves' that may allow for a greater proportion of Th to be sourced from bedrock to impact the zero-age calcite measured here. This source was not characterized as part of this study. The Edwards Group Limestones and Cow Creek Formation, in which the cave sites described here reside, includes 1) the argillaceous Georgetown Fm. that is stratigraphically above NB and IS and has undergone chertification (Abbott, 1975), 2) the Glen Rose formation with argillaceous units (Golab et al., 2017) above NB, and 3) the Hensel Formation with basal fluviatile or estuarine clays (Stricklin Jr. and Smith, 1973) above WC. The clay in these units may contribute to the elevated <sup>230</sup>Th/<sup>232</sup>Th in the zero-age calcite measured here. Furthermore, chert in the Edwards Group Limestones has a Th concentration of 0.01 to 2.29 ppm (Speer, 2014; personal communication). We note, however, that the half-life of  $^{230}$ Th ( $\sim$ 75 ka) and the resistance of chert to weathering, may limit the contribution of these bedrock sources to zero-age calcite. Additionally, some caves in central Texas, including IS, have a relict soil within them that is no longer above the cave today and is potentially derived from the Del Rio Clay (Toomey et al., 1993; Cooke et al., 2007). More measurements of <sup>230</sup>Th/<sup>232</sup>Th in cave dust, host bedrock, and in dripwater could help constrain the sources of detrital <sup>230</sup>Th/<sup>232</sup>Th in NB and IS.

Ammonium acetate leachates of the soils from all three caves have lower concentrations of <sup>232</sup>Th, <sup>230</sup>Th, Fe, and Mn than the DI water leachates from the same soil samples (Fig. 4; Table 2). Leaching with ammonium acetate buffered to pH 8 is hypothesized to readily strip exchangeable cations from soils (e.g., Harrison et al., 1989). DI water, by contrast, would allow for characterization of the elements within soil pore waters, loosely bound to mineral surfaces, and salts within the soils alone (McLaren et al., 1998). DI water, and thus rainwater, is likely a more aggressive solvent based on the results of this study (pH 7.57) and may leach some acid labile material from the soil that is not in pore water or in salts. Buffering from the calcite in the soil, however, may dampen the effect (Lee and Touray, 1998). Moreover, the <sup>230</sup>Th/<sup>232</sup>Th values of both leachate types on the same samples agree within uncertainty at all three caves (Supp. Fig. 1). Consequently, we suggest that the leach types may be sampling from the same sources of Th in the soils and that the DI water is more efficient at leaching these components than the ammonium acetate.

# 6. Conclusions and recommendations

We monitored and analyzed calcite growth at five dripwater sites in three caves in central Texas to determine the concentration of detrital  $^{230}\mathrm{Th}$  in zero-age calcite.  $^{230}\mathrm{Th}/^{232}\mathrm{Th}$  values are elevated in zero-age calcite and soil relative to the bulk earth value (4.4 ppm) that is commonly used to correct measured U-series ages. The results from the soil analysis suggest that soil is a contributor to detrital Th in calcite at the cave sites studied here. The zero-age calcite  $^{230}\mathrm{Th}/^{232}\mathrm{Th}$  values (5.4 to 28.1 ppm) are similar to detrital  $^{230}\mathrm{Th}/^{232}\mathrm{Th}$  values from central Texas as previously determined using stalagmite isochrons (14.7 to 20.7 ppm) and modeled using a < 100-year-old stalagmite from WC (3.9 to 11.2 ppm). We conclude that the bulk earth value is not an accurate proxy for the detrital Th used in U-series age determinations for many central Texas speleothems. We recommend:

- 1. For speleothems with a low U content, that are "dirty", or that are particularly young we suggest that the zero-age calcite method should be considered to correct the U-series ages as opposed to the bulk earth assumption. We recognize that this method can only be applied in locations where caves can be monitored. Given the extensive network of cave monitoring studies globally (e.g., Baker et al., 2019), however, this method may be useful to many researchers. Furthermore, applying this method to correct for detrital 230Th/232Th in appropriate speleothems may reduce the bias against dirty speleothems in the global paleoclimate record.
- 2. The zero-age calcite method outlined here helps access the sources and fluxes of detrital <sup>230</sup>Th in a cave system. Consequently, we recommend monitoring cave environments across seasons and decadal periods to help characterize the detrital Th flux and isotopic ratios as they relate to climate. For example, analyzing zero-age calcites from substrates collected in the 18-year monitoring studies in central Texas (e.g., Banner et al., 2007; Feng et al., 2014) would lead to improvements in U-series age models for stalagmites from the region and would improve our understanding of the processes that control variations in <sup>230</sup>Th/<sup>232</sup>Th values in stalagmite calcite.
- 3. We note that speleothems that have a high concentration of uranium and are relatively "clean" of detrital content are not the intended target for this method. In these cases, bulk earth assumptions, or estimates of detrital <sup>230</sup>Th/<sup>232</sup>Th based on other data, do not contribute significantly to the U-series age determined or its uncertainty.

#### **Declaration of Competing Interest**

The authors declare that they have no known competing financial interests or personal relationships that could have appeared to influence the work reported in this paper.

#### Acknowledgements

We would like to acknowledge the NSF Research Experience for Undergraduates (EAR-1157031) hosted by the Environmental Science Institute at University of Texas at Austin that supported B.E.W. in 2012. Additionally, we would like to acknowledge support from the F. M. Bullard Professorship of the Jackson School of Geosciences.

# Appendix A. Supplementary data

Supplementary data to this article can be found online at https://doi.org/10.1016/j.palaeo.2022.110978.

# References

Abbott, P.L., 1975. On the hydrology of the Edwards Limestone, south-Central Texas. J. Hydrol. 24 (3–4), 251–269. https://doi.org/10.1016/0022-1694(75)90084-0.

Baker, A., Hartmann, A., Duan, W., Hankin, S., Comas-Bru, L., Cuthbert, M.O., Treble, P. C., Banner, J.L., Genty, D., Baldini, L.M., Bartolome, M., 2019. Global analysis reveals climatic controls on the oxygen isotope composition of cave drip water. Nature Comm. 10 (1), 1–7.

Baker, A., Smart, P.L., Edwards, R.L., Richards, D.A., 1993. Annual growth banding in a cave stalagmite. Nature. 364, 518–520. https://doi.org/10.1038/364518a0.

Baker, A., Barnes, W.L., Smart, P.L., 1997. Variations in the discharge and organic matter content of stalagmite drip waters in lower Cave. Bristol. Hydro. Proc. 11, 1541–1555. https://doi.org/10.1002/(SICI)1099-1085(199709)11:11<1541::AID-HYP484>3.0.C0:2-7.

Baker, A., Genty, D., Dreybrodt, W., Barnes, W.L., Mockler, N.J., Grapes, J., 1998.
Testing theoretically predicted stalagmite growth rate with recent annually laminated samples: implications for past stalagmite deposition. Geochim.
Cosmochim. Acta 62 (3), 393–404. https://doi.org/10.1016/S0016-7037(97)00343-

Banner, J.L., Guilfoyle, A., James, E., Stern, L.A., Musgrove, M., 2007. Seasonal variations in modern speleothem calcite growth in Central Texas, U.S.A. J. Sediment. Res. 77, 615–622.

Birdwell, J.E., Engel, A.S., 2009. Variability in terrestrial and microbial contribution to dissolved organic matter fluorescence in the Edwards aquifer, Central Texas. J. Cave Karst Stud. 71 (2), 144–156.

- Blyth, A.J., Fuentes, D., George, S.C., Volk, H., 2015. Characterisation of organic inclusions in stalagmites using laser-ablation-micropyrolysis gas chromatographymass spectrometry. J. Anal. Appl. Pyrolysis 113, 454–463. https://doi.org/10.1016/ i.jaap.2015.03.009
- Bohn, H.L., Myer, R.A., O'Connor, G.A., 1985. Soil Chemistry, Second edition. John Wiley & Sons, New York.
- Cai, Y., Chiang, J.C., Breitenbach, S.F., Tan, L., Cheng, H., Edwards, R.L., An, Z., 2017. Holocene moisture changes in western China, Central Asia, inferred from stalagmites. Quat. Sci. Rev. 158, 15–28.
- Carlson, P.E., Banner, J.L., Johnson, K.R., Casteel, R.G., Breecker, D.O., 2019. Carbon cycling of subsurface organic matter recorded in speleothem 14C records: Maximizing bomb-peak model fidelity. Geochim. Cosmochim. Acta 246, 436–449.
- Carlson, P.E., Miller, N.R., Banner, J.L., Breecker, D.O., Casteel, R.C., 2018. The potential of near-entrance stalagmites as high-resolution terrestrial paleoclimate proxies: Application of isotope and trace-element geochemistry to seasonally resolved chronology. Geochim. Cosmochim. Acta 235, 55–75. https://doi.org/10.1016/j. gca.2018.04.036.
- Carolin, S.A., Cobb, K.M., Lynch-Stieglitz, J., Moerman, J.W., Partin, J.W., Lejau, S., Malang, J., Clark, B., Tuen, A.A., Adkins, J.F., 2016. Northern Borneo stalagmite records reveal West Pacific hydroclimate across MIS 5 and 6. Earth Planet. Sci. Lett. 430, 122, 103
- Casteel, R.C., 2011. The Modern Assessment of Climate, Calcite Growth, and the Geochemistry of Cave Drip Waters as a Precursor to Paleoclimate Study. Dissertation. The University of Texas at Austin. http://hdl.handle.net/2152/ ETD-UT-2011-08-4177.
- Casteel, R.C., Banner, J.L., 2015. Temperature-driven seasonal calcite growth and drip water trace element variations in a well-ventilated Texas cave: Implications for speleothem paleoclimate studies. Chem. Geol. 392, 43–58. https://doi.org/10.1016/ i.chemgeo.2014.11.002.
- Cheng, H., Edwards, R.L., Hoff, J., Gallup, C.D., Richards, D.A., Asmerom, Y., 2000. The half-lives of uranium-234 and thorium-230. Chem. Geol. 169, 17–33.
- Cheng, H., Edwards, R.L., Shen, C.C., Polyak, V.J., Asmerom, Y., Woodhead, J., Hellstrom, J., Wang, Y., Kong, X., Spotl, C., Wang, X., Alexander Jr., E.C., 2013. Improvements in 230Th dating, 230Th and 234U half-life values, and U-Th isotopic measurements by multi-collector inductively coupled plasma mass spectrometry. Earth Planet. Sci. Lett. 371-372, 82–91.
- $\label{lem:continuous} Climate \ Prediction \ Center \ (CPC), \ 2015. \ National \ Weather Service. \ U.S. \ Drought \ Monitor. \\ https://www.cpc.ncep.noaa.gov/products/Drought/.$
- Cooke, M.J., Stern, L.A., Banner, J.L., Mack, L.E., 2007. Evidence for the silicate source of relict soils on Edwards Plateau, Central Texas. Ouat. Res. 67, 275–285.
- Cowan, B.D., Osborne, M.C., Banner, J.L., 2013. Temporal variability of cave air CO2 in Central Texas. J. Cave Karst Stud. 75 (1), 38–50.
- Denniston, R.F., Wyrwoll, K.-H., Asmerom, Y., Polyak, V.J., Humphreys, W.F., Cugley, J., Woods, D., LaPointe, Z., Peota, J., Greaves, E., 2013. North Atlantic forcing of millennial-scale Indo-Australian monsoon dynamics during the last Glacial period. Quat. Sci. Rev. 72, 159–168. https://doi.org/10.1016/j.quascirev.2013.04.012.
- Dorale, J.A., Edwards, R.L., Alexander Jr., C.E., Shen, C.-C., Richards, D.A., Cheng, H., 2004. Uranium-Series Dating of Speleothems: Current Techniques, Limits, and Applications. Studies of Cave Sediments. pp. 177–197.
- Applications. Studies of Cave Sediments, pp. 177–197. Edwards, R.L., Chen, J.H., Wasserburg, G.J., 1987. 238U-234U-230Th-232Th systematics and the precise measurement of time over the past 500,000 years. Earth Planet. Sci. Lett. 81, 175–192.
- Edwards, R.L., Beck, J.W., Burr, G.S., Donahue, D.J., Chappell, J.M.A., Bloom, A.L., Druffel, E.R.M., Taylor, F.W., 1993. A large drop in atmospheric 14C/12C and reduced melting in the Younger Dryas, document with 230Th ages of corals. Science. 260 (5110), 962–968.
- Elliot, W.R., Veni, G., 1994. The Caves and Karst of Texas: Huntsville. National Speleological Society, Convention Guidebook, p. 342.
- Feng, W., Casteel, R.C., Banner, J.L., Heinz-Fry, A., 2014. Oxygen isotope variations in rainfall, drip-water, and speleothem calcite from a well-ventilated cave in Texas, USA: Assessing a new speleothem temperature proxy. Geochim. Cosmochim. Acta 127, 233–250.
- Golab, J.A., Smith, J.J., Clark, A.K., Morris, R.R., 2017. Bioturbation-influenced fluid pathways within a carbonate platform system: the lower cretaceous (Aptian-Albian) Glen Rose Limestone. Paleogeogr. Paleoclimatol. Paleoecol. 465 (A), 138–155.
- Hardt, B., Rowe, H.D., Springer, G.S., Cheng, H., Edwards, R.L., 2010. The seasonality of east central North American precipitation based on three coeval Holocene speleothems from southern West Virginia. Earth Planet. Sci. Lett. 295 (3–4), 342–348
- Harrison, R.B., Johnson, D.W., Todd, D.E., 1989. Sulfate adsorption and desorption reversibility in a variety of forest soils. J. Environ. Qual. 18, 419–426. https://doi. org/10.2134/jeq1989.00472425001800040004x.
- Hellstrom, J., 2006. U-Th dating of speleothems with high detrital 230Th using stratigraphical constraint. Quat. Geochronol. 1, 289–295.
- Huang, Y., Fairchild, I.J., Borsato, A., Frisia, S., Cassidy, N.J., McDermott, F., Hawkesworth, C.J., 2001. Seasonal variations in Sr, Mg and P in modern speleothems (Grotta di Ernesto, Italy). Chem. Geol. 175 (3–4), 429–448.
- Hulewicz, M., 2012. Physical and geochemical response in cave drip waters to recent drought, central Texas, USA: implications for drought reconstruction using speleothems. Masters Thesis.
- James, C.D., 2017. A Central Texas Drying Event Identified at the Younger Dryas-Early Holocene Transition Using Coupled Speleothem d13C-14C Analysis. Thesis. The University of Texas at Austin. http://hdl.handle.net/2152/64615.
- James, E.W., Banner, J.L., Hardt, B., 2015. A global model for cave ventilation and seasonal bias in speleothem paleoclimate records. Geochm. Geophys. Geosys. 16 (4), 1044–1051. https://doi.org/10.1002/2014GC005658.

- Kastning, E.H., 1983. Relict caves as evidence of landscape and aquifer evolution in a deeply dissected carbonate terrain: southwest Edwards Plateau, Texas, USA. J. Hydrol. 61 (1–3), 89–112.
- Kaufman, A., Wasserburg, G.J., Porcelli, D., Bar-Matthews, M., Ayalon, A., Halicz, L., 1998. U-Th isotope systematics from the Soreq cave, Israel and climatic correlations. Earth Planet. Sci. 156 (3-4), 141–155. https://doi.org/10.1016/S0012-821X(98)
- Labonne, M., Hillaire-Marcel, C., Ghaleb, B., Goy, J.-L., 2002. Multi-isotopic age of dirty speleothem calcite: an example from Altamira Cave, Spain. Quat. Sci. Rev. 21, 1099–1110.
- Lachniet, M.S., Asmerom, Y., Burns, S.J., Patters, W.P., Polyak, V.J., Seltzer, G.O., 2014. Tropical response to the 8200 yr B.P. cold event? Speleothem isotopes indicate a weakened early Holocene monsoon in Costa Rica. Geology 32 (11), 957–960.
- Larkin, T.J., Bomar, G.W., 1983. Climatic Atlas of Texas. Texas Department of Water Resources, p. 151.
- Lee, P.-K., Touray, J.-C., 1998. Characteristics of a polluted artificial soil located along a motorway and effects of acidification on the leaching behavior of heavy metals (Pb, Zn, Cd). Water Res. 32 (11), 3425–3435. https://doi.org/10.1016/S0043-1354(98) 00110-9.
- Lin, J.C., Broecker, W.S., Anderson, R.F., Hemming, S., Rubenstone, J.L., Bonani, G., 1996. New 230Th/U and 14C ages from Lake Lahontan carbonates, Nevada, USA, and a discussion of the origin of detrital thorium. Geochim. Cosmochim. Acta 60 (15), 2817–2832.
- Ludwig, K.R., Paces, J.B., 2002. Uranium-series dating of pedogenic silica and carbonate, Crater flat, Nevada. Geochim. Cosmochim. Acta 66 (3), 487–506.
- Mahler, B.J., Lynch, F.L., 1999. Muddy waters: temporal variation in sediment discharging from a karst spring. J. Hydro. 214, 165–178. https://doi.org/10.1016/ S0022-1694(98)00287-X.
- McDermott, F., 2004. Palaeo-climate reconstruction from stable isotope variations in speleothems: a review. Quat. Sci. Rev. 23 (7–8), 901–918.
- McLaren, R.G., Backes, C.A., Rate, A.W., Swift, R.S., 1998. Cadmium and cobalt desorption kinetics from soil clays: effect of sorption period. Soil Sci. Soc. Am. J. 62, 332–337. https://doi.org/10.2136/sssaj1998.03615995006200020006x.
- Meckler, A.N., Clarkson, M.O., Cobb, K.M., Sodemann, H., Adkins, J.F., 2012.
  Interglacial hydroclimate in the tropical West Pacific through the late Pleistocene.
  Science. 336 (6086), 1301–1304. https://doi.org/10.1126/science.1218340.
- Meckler, A.N., Affolter, S., Dublyansky, Y.V., Kruger, Y., Vogel, N., Vernasconi, S.M., Frenz, M., Kipfer, R., Leuenberger, M., Spotl, C., Carolin, S., Cobb, K.M., Moerman, J., Adkins, J.F., Fleitman, D., 2015. Glacial-interglacial temperature change in the tropical West Pacific: a comparison of stalagmite-based paelothermometers. Quat. Sci. Rev. 127, 90–116. https://doi.org/10.1016/j.guascirev.2015.06.015.
- Morton, L.W., Evans, C.V., Harbottle, G., Estes, G.O., 2001. Pedogenic fractionation and bioavailability of uranium and thorium in naturally radioactive spodosols. Soil Sci. Soc. Am. J. 65. 1197–1203.
- Moseley, G., Spötl, C., Svensson, A., Cheng, H., Bradstätter, S., Edwards, R.L., 2014. Multi-speleothem record reveals tightly coupled climate between central Europe and Greenland during Marine Isotope Stage 3. Geology 42 (12), 1043–1046. https://doi. org/10.1130/G36063.1.
- Musgrove, M., Banner, J.L., 2004. Controls on the spatial and temporal variability of vadose dripwater geochemistry: Edwards Aquifer, Central Texas. Geochim. Cosmochim. Acta 68, 1007–1020.
- Musgrove, M., Banner, J.L., Mack, L.E., Combs, D.M., James, E.W., Cheng, H., Edwards, R.L., 2001. Geochronology of late Pleistocene to Holocene speleothems from Central Texas: Implications for regional paleoclimate. GSA Bull. 113 (12), 1532–1543.
- Nascimento, R.C., da Silva, Y.J.A.B., do Nascimento, C.W.A., da Silva, Y.J.A.B., da Silva, R.J.A.B., Collins, A.L., 2019. Thorium content in soil, water and sediment samples and fluvial sediment-associated transport in a catchment system with a semiarid-coasta interface. Brazil. Enivorn. Sci. Pollut. Res. 26, 33532–33540. https://doi.org/10.1007/s11356-019-06499-8.
- Novello, V.F., Cruz, F.W., Karmann, I., Burns, S.J., Stríkis, N.M., Vuille, M., et al., 2012. Multidecadal climate variability in Brazil's Nordeste during the last 3000 years based on speleothem isotope records. Geophys. Res. Lett. 39 (23), L23706. https://doi.org/10.1029/2012GL053936.
- Orland, I.J., Burstyn, Y., Bar-Matthews, M., Kozdon, R., Ayalon, A., Matthews, A., Valley, J.W., 2014. Seasonal climate signals (1990–2008) in a modern Soreq Cave stalagmite as revealed by high-resolution geochemical analysis. Chem. Geol. 363, 322–333.
- Oster, J.L., Ibarra, D.E., Harris, C.R., Maher, K., 2020. Influence of eolian deposition and rainfall amounts on the U-isotopic composition of soil water and soil minerals. Geochim. Cosmochim. Acta 88, 146–166.
- Polyak, V.J., Rasmussen, J.B.T., Asmerom, Y., 2004. Prolonged wet period in southwestern United States through the Younger Dryas. Geology. 32 (1), 5–8.
- PRISM Climate Group, 2015a. 30-yr Normal Mean Average Temperature: Annual. Period, pp. 1981–2010. Available at: http://prism.oregonstate.edu/. Accessed on: August 3, 2015.
- PRISM Climate Group, 2015b. 30-yr Normal Mean Average Rainfall: Annual. Period, pp. 1981–2010. Available at: http://prism.oregonstate.edu/. Accessed on: August 3, 2015.
- Przybylowicz, W., Schwarcz, H.P., Latham, A.G., 1991. Dirty calcites 2. Uranium-series dating of artificial calcite-detritus mixtures. Chem. Geol.: Isotope Geosci. Sect. 86 (2), 161–178.
- Rachkova, N.G., Shuktomova, I.I., Taskaev, A.I., 2010. The state of natural radionuclide of uranium, radium, and thorium in soils. Eurasian Soil Sci. 43 (6), 651–658.

- Reiller, P., Moulin, V., Casanova, F., Dautel, C., 2002. Retention and behaviour of humic substances onto mineral surfaces and consequences upon thorium (IV) mobility: case of iron oxides. App. Chem. 17, 1551–1562.
- Richards, D.A., Dorale, J.A., 2003. Uranium-series chronology and environmental applications of speleothems. Rev. Mineral. Geochem. 52 (1), 407–460. https://doi. org/10.2113/0520407.
- Richards, D.A., Bottrell, S.H., Cliff, R.A., Strohle, K., Rowe, P.J., 1998. U-Pb dating of a speleothem of Quaternary age. Geochim. Cosmochim. Acta 62 (23/24), 3683–3688.
- Schwarcz, H.P., Latham, A.G., 1989. Dirty calcites: 1. Uranium-series dating of contaminated calcite using leachates alone. Chem. Geol. 80, 35–43.
- Scroxton, N., Gagan, M.K., Dunbar, G.B., Ayliffe, L.K., Hantoro, W.S., Shen, C.-C., Hellstrom, J.C., Zhao, J.-x., Cheng, H., Edwards, R.L., Sun, H., Rifai, H., 2016. Natural attrition and growth frequency variations of stalagmites in southwest Sulawesi over the past 530,000 years. Paleogeogr. Paleclimatol. Paleoecol. 441 (4), 823–833.
- Shen, C.-C., Edwards, R.L., Cheng, H., Dorale, J.A., Thomas, R.B., Moran, S.B., Weinstein, S.E., Edmonds, H.N., 2002. Uranium and thorium isotopic and concentration measurements by magnetic sector inductively coupled plasma mass spectrometry. Chem. Geol. 185, 165–178.
- Speer, C.A., 2014. Experimental sourcing of Edwards Plateau chert using LA-ICP-MS. Quat. Int. 342, 199–213. https://doi.org/10.1016/j.quaint.2014.03.030.
- Steponaitis, E., Andrews, A., McGee, D., Quade, J., Hsieh, Y.T., Broecker, W.S., et al., 2015. Mid-Holocene drying of the US Great Basin recorded in Nevada speleothems. Quat. Sci. Rev. 127, 174–185.
- Stricklin Jr., F.L., Smith, C.I., 1973. Environmental reconstruction of a carbonate beach complex: Cow Creek (lower cretaceous) formation of Central Texas. GSA Bull. 84, 1349–1368.
- Taylor, S.R., McLennan, S.M., 1995. The geochemical evolution of the continental crust. Rev. Geophys. 33 (2), 241–265. https://doi.org/10.1029/95RG00262.

- Toomey, R.S., Blum, M.D., Valastro Jr., S., 1993. Late Quaternary climates and environments of the Edwards Plateau, Texas. Glob. Planet. Chang. 7 (4), 299–320. https://doi.org/10.1016/0921-8181(93)90003-7.
- Wagner, J., Cole, J., Beck, J., et al., 2010. Moisture variability in the southwestern United States linked to abrupt glacial climate change. Nature Geosci. 3, 110–113. https://doi.org/10.1038/ngeo707.
- Wang, J., Liu, J., Li, H., Chen, Y., Xiao, T., Song, G., Chen, D., Wang, C., 2017. Uranium and thorium leachability in contaminated stream sediments from a uranium minesite. J. Chem. Explor. 176, 85–90. https://doi.org/10.1016/j.gexplo.2016.01.008.
- Wedepohl, K.H., 1995. The composition of the continental-crust. Geochim. Cosmochim. Acta 59, 1217–1232. https://doi.org/10.1016/0016-7037(95)00038-2.
- Wendt, K.A., Li, X., Edwards, R.L., 2021. Uranium-Thorium dating of speleothems. Elements. 17 (2), 87–92.
- White, W.B., Brennan, E.S., 1989. Luminescence of speleothems due to fulvic acid and other activators. In: Proceedings of the 10th International Congress of Speleology, Budapest, Hungary, pp. 212–214.
- Wong, C.I., Breecker, D.O., 2015. Advancements in the use of speleothems as climate archives. Quat. Sci. Rev. 127, 1–18.
- Wong, C.I., Banner, J.L., Musgrove, M., 2011. Seasonal dripwater Mg/Ca and Sr/Ca variations driven by cave ventilation: Implications for and modeling of speleothem paleoclimate records. Geochim. Cosmochim. Acta 75, 3514–3529.
- Wong, C.I., Musgrove, M., Banner, J.L., 2015. Holocene climate variability in Texas, USA: An integration of existing paleoclimate data and modeling with a new, highresolution speleothem record. In: Quaternary Science Reviews. In Press.
- Xiu, T., Liu, Z., Wang, Y., Wu, P., Du, Y., Cai, Z., 2019. Thorium adsorption on graphene oxide nanoribbons/manganese dioxide composite material. J. Radioanal. Nucl. Chem. 319, 1059–1067.
- Zhao, J.-x., Yu, K.-f., Feng, Y.-X., 2009. High-precision 238U–234U-230Th disequilibrium dating of the recent past: a review, 4, pp. 423–433.